

Low-noise solar-blind photodetectors based on LaAlO_3 single crystal with transparent indium-tin-oxide electrode as detection window

Er-Jia Guo, Hui-Bin Lu,* Meng He, Kui-Juan Jin, and Guo-Zhen Yang

Beijing National Laboratory for Condensed Matter Physics, Institute of Physics,
Chinese Academy of Sciences, Beijing 100190, China

*Corresponding author: hblu@aphy.iphy.ac.cn

Received 1 July 2010; revised 10 September 2010; accepted 13 September 2010;
posted 14 September 2010 (Doc. ID 130949); published 8 October 2010

The low-noise solar-blind photodetectors of indium-tin-oxide/ LaAlO_3 /Ag (ITO/LAO/Ag) have been fabricated based on the properties of LAO bandgap excitation and the transparent conductance of ITO thin film. The ITO thin films are epitaxially grown on LAO wafers as the electrodes and detection windows of the photodetectors. The photodetectors have low noise and excellent electromagnetic shielding. The influence of the thickness of ITO thin films on the responsivity of the photodetectors has been studied. The photocurrent responsivity can reach 10.3 mA/W under the irradiation of 200–220 nm for a photodetector with 5 nm thick ITO film. The noise current is 1 pA order magnitude under the sunlight at midday. The experiment results suggest that ITO/LAO/Ag is one of the promising structures for the solar-blind deep-ultraviolet photodetectors. © 2010 Optical Society of America

OCIS codes: 040.5150, 040.5160, 040.7190, 310.7005.

1. Introduction

Solar-blind deep-ultraviolet (DUV) photodetectors with excellent thermal stability and reliability have attracted much attention due to their various potential applications in the fields of solar astronomy, short-range communications security, space-to-space transmission, fire alarms, combustion monitoring, and military services. Solar-blind DUV detectors can work in a harsh environment of sunlight radiation, especially. Therefore, there has been great interest in the development of solar-blind photodetectors with various wide bandgap materials in the past few years, such as $\text{Al}_x\text{Ga}_{1-x}\text{N}$ [1–3], cBN [4], diamond [5,6], MgZnO [7], and others. Recently, we reported the solar-blind photodetectors of LaAlO_3 [8] and LiTaO_3 [9] single crystals with Au-interdigitated electrodes based on very good chemical and thermal stability. Although the photodetectors of LaAlO_3 and LiTaO_3 have high DUV sensitivities of 71.8 and

2 mA/W and low dark currents of 77 and 61 pA, respectively, from the view of practical applications, there are some problems with the structure of interdigitated electrodes. One of the problems is that the ability of anti-interference is not good enough for the electromagnetic interferences of detection space. On the other hand, for the detectors with interdigitated electrodes, one must add a window in the front of the detector chip to avoid contaminants such as dust or conductive particles in the detection circumstance. In this paper, we report the low-noise solar-blind photodetectors of indium-tin-oxide/ LaAlO_3 /Ag (ITO/LAO/Ag) based on the properties of LAO bandgap excitation and the transparent conductance of ITO thin film.

Figure 1 shows the schematic diagram of the ITO/LAO/Ag photodetectors. ITO thin films as transparent electrodes have been widely used in panel displays, solar cells, and optoelectronics due to their low electrical resistivity and high transparency [10–12]. The ITO thin film is epitaxially grown on a surface of LAO as an electrode and the detection window.

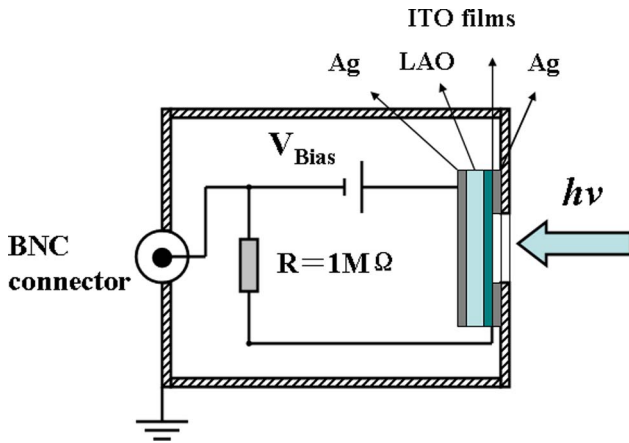


Fig. 1. (Color online) Schematic diagram of ITO/LAO/Ag photodetector.

In order to improve the ability of the electromagnetic shield, the ITO film is connected with the cavity using Ag glue. The other surface of LAO is smeared with Ag glue uniformly as another electrode. Because the ITO films have a good metalliclike property, the structure of the photodetector chip is a typical metal(ITO)-insulator(LAO)-metal(Ag) structure. The detector chip and sampling resistance, $R = 1 \text{ M}\Omega$, are installed in an Al cavity. In this way, the photodetector has low noise and a very good electromagnetic shield. As shown in Fig. 1, the diameter of the detection window is 4 mm, corresponding to the efficient area of the photodetectors, 12.56 mm^2 . The mechanism of photocurrent for the ITO/LAO/Ag photodetectors, similar to the LAO photodetectors with interdigitated electrodes [8], can be understood as the following: the incident light passes through the ITO thin film and comes into the LAO single crystal. The LAO absorbs the incident photons and generates the photocarriers (electron-hole pairs) when the photon energies are higher than the bandgap of LAO. The photogenerated electrons and holes are separated by the electric field of supplied bias and form the photocurrent.

2. Experimental Details

The LAO wafers used in the present study are as-supplied commercial LAO single crystal with a purity of 99.99% and a single polished mirror. The geometry size of the LAO wafers is $5 \text{ mm} \times 10 \text{ mm}$ with a thickness of 0.5 mm. As mentioned in our previous works [13], we epitaxially grow ITO thin films on LAO wafers by a laser molecular-beam epitaxy system. The preparation conditions of ITO thin films are as follows: a sintered ceramic ITO ($\text{In}_2\text{O}_3 : \text{SnO}_2 = 90 : 10 \text{ wt.}\%$) is used as the target, the laser beam with a wavelength of 308 nm has a repetition rate of 2 Hz and a duration of 25 ns, the laser energy density is approximately 1.5 J/cm^2 , the temperature of LAO substrates is kept at $680 \text{ }^\circ\text{C}$, and an oxygen pressure of $1.5 \times 10^{-1} \text{ Pa}$ is maintained during the deposition. After the deposition, the samples were *in situ* annealing under the growth conditions for 30 min. ITO thin films with different

thicknesses of 5, 20, and 100 nm are deposited on LAO substrates, respectively. The thicknesses of ITO thin films are controlled by the intensity oscillations of an *in situ* reflection high-energy electron diffraction and further confirmed by a surface profile measuring system.

3. Results and Discussion

Figure 2 presents a typical x-ray diffraction (XRD) $\theta \sim 2\theta$ scan curve of a 100 nm-thick ITO thin film on LAO. Except for the ITO (00 l) and LAO (00 l) diffraction peaks, there is no other diffraction peak from impurity phases or a randomly oriented grain, indicating that ITO thin film is single phased and epitaxially grown on LAO. The Hall measurements confirmed that the resistivities of ITO are 9.46×10^{-2} , 2.75×10^{-3} , and $1.43 \times 10^{-4} \text{ }\Omega \cdot \text{cm}$ for 5, 20, and 100 nm thin films, respectively. All of the ITO films have a good epitaxial structure, and the interfaces between LAO and ITO are very sharp. The relative property with structure will be reported elsewhere.

We studied the influence of the thickness of ITO thin films on the responsivity of the photodetectors. In order to improve the responsivity, at first, we polished all of the LAO wafers with different ITO thicknesses of 5, 20, and 100 nm mechanically into 0.13 mm. A tunable DC voltage source is taken as the applied source. A 30 W D_2 lamp is employed to act as a light source, and the light intensity is calibrated by a UV-enhanced silicon photodetector in the wavelength range of 200–220 nm. The photovoltages across the sampling resistance R are measured by a 500 MHz oscilloscope. The noise currents are measured using a Keithley Model 2400 source meter.

Figure 3 shows the bias dependence of the photocurrent responsivities for the three different photodetectors with 5, 20, and 100 nm ITO thin films under the irradiation of a D_2 lamp, respectively. The photocurrent responsivities increase linearly with applied bias for all three photodetectors.

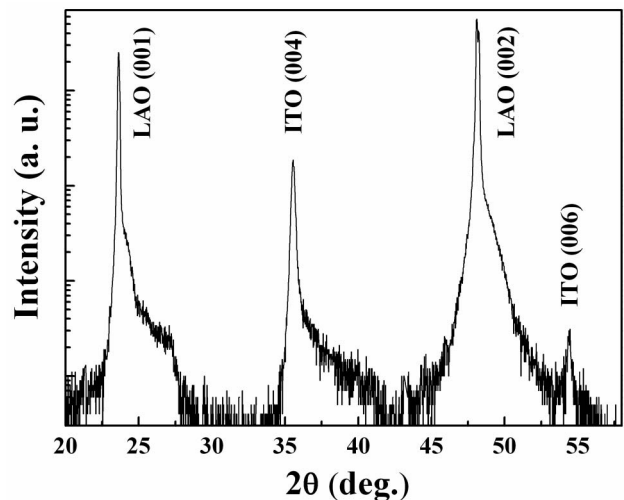


Fig. 2. Typical XRD $\theta - 2\theta$ scan curve of 100 nm ITO film on LAO substrate.

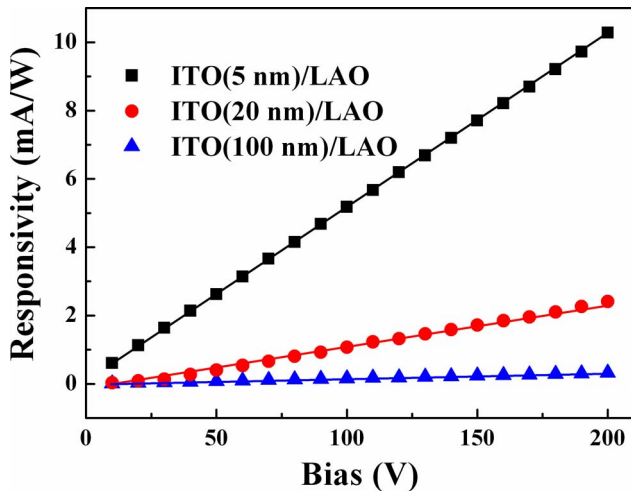


Fig. 3. (Color online) Bias dependence of the photocurrent responsivity for the three different photodetectors with 5, 20, and 100 nm ITO films under the irradiation of a D_2 lamp.

The maximum responsivities are 0.3, 2.4, and 10.3 mA/W at 200 V bias for the photodetectors with 100, 20, and 5 nm ITO thin films, respectively. It is obvious that the responsivity decreases rapidly with the increase of the thickness of ITO thin films, indicating that the thickness of ITO thin film has a larger influence for the photocurrent responsivity.

Figure 4 presents the optical transmittances of ITO thin films with the thicknesses of 5, 20, and 100 nm, respectively. The 100 nm ITO thin film shows a sharp cutoff wavelength at about 320 nm, agreeing well with the ITO bandgap of 3.8 eV [10]. Therefore, with the increase of the thickness of ITO film, the absorption of UV light in ITO film increased. As we know, the absorption of ITO film is disadvantageous to the detection responsivity because the electron-hole pairs generated by the absorption of ITO film will be recombined quickly due

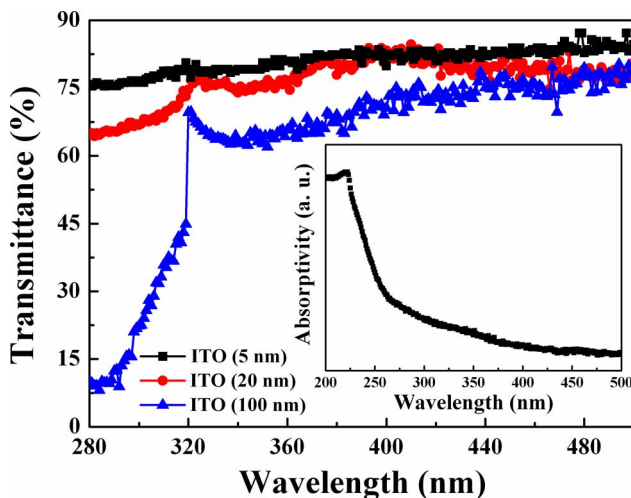


Fig. 4. (Color online) Optical transmittances of ITO films with the different thickness of 5, 20, and 100 nm. The inset shows the absorption spectrum of an LAO single crystal with 5 nm thick ITO film.

to the metalliclike property of ITO films. From Fig. 4, we can see that the transmittances are about 9%, 63%, and 76% in the 280 nm wavelength for the 100, 20, and 5 nm ITO films, respectively. In Fig. 3, the LAO with 100 nm ITO film has the lower responsivity since the most incidence light was absorbed by the ITO film and only less incidence light can reach LAO, and vice versa, the LAO with 5 nm ITO film has the higher responsivity.

The inset of Fig. 4 shows the absorption spectrum of a LAO single crystal with 5 nm thick ITO film. The absorption spectrum is agreeing well with that of LAO photodetectors with interdigitate electrodes [8]. The cutoff wavelength of the spectrum is at about 220 nm corresponding to a photon energy of 5.6 eV [14], agreeing well with the LAO bandgap. The experimental results prove that the 5 nm thick ITO film has almost no influence for the spectral characteristics of LAO photoresponse, and the ITO/LAO/Ag photodetectors have an intrinsic characteristic of solar blindness.

Figure 5 shows the power density dependence of the photocurrent for a ITO/LAO/Ag photodetector with 5 nm ITO film under the irradiation of a D_2 lamp at a 200 V bias. The photocurrent presents a good linear relationship with the power density. From Fig. 5, it can be seen that the photodetector can detect the incidence light as low as $0.09 \mu\text{W}/\text{cm}^2$ or even smaller. The dark current is about 1 pA at 200 V bias, indicating that the photodetector has a low noise and the excellent electromagnetic shielding. As shown in the inset of Fig. 5, we also measured the noise currents directly under sunlight with a light intensity of $\sim 100 \text{ mW}/\text{cm}^2$. The noise currents of a photodetector with 5 nm ITO are 10, 55, 187, and 536 pA at 10, 50, 100, and 200 V bias, respectively. The noise currents are bigger than the dark current. The reason for arousing the bigger noise currents may be that the LAO used in our experiment is not perfect. However, the noise currents are pA magnitude. The result

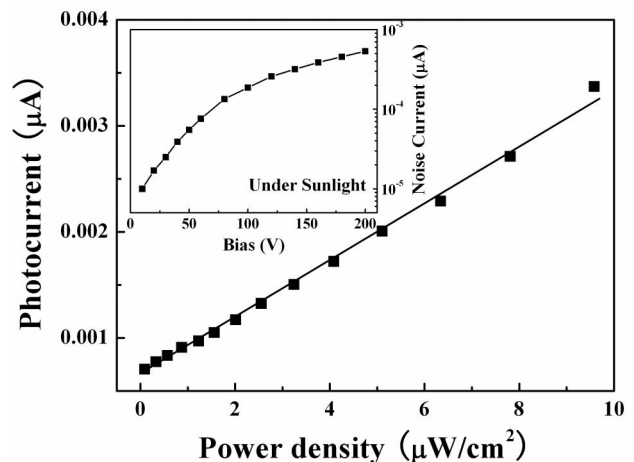


Fig. 5. Power density dependence of the photocurrent for an ITO/LAO/Ag photodetector with 5 nm ITO film under the irradiation of a D_2 lamp at a 200 V bias. The inset shows the bias dependence of noise currents under the irradiation of sunlight at midday.

suggests that the ITO/LAO/Ag photodetector can directly detect the DUV light without any filter under sunlight.

4. Conclusions

In conclusion, we have successfully fabricated the low-noise solar-blind photodetectors of ITO/LAO/Ag. The photodetectors have a very low noise and excellent electromagnetic shielding. The photocurrent responsivity reaches 10.3 mA/W under the irradiation of 200–220 nm. The noise current is 1 pA order of magnitude under the sunlight at midday. The responsivity, though, is not higher than that of LAO photodetectors with interdigitated electrodes, as we reported previously [8]. However, in the view of application, the MIM structured photodetectors have more wide application due to the excellent electromagnetic shielding as well as the sufficient responsivity. In addition, the present photodetectors can be improved by further decreasing the thickness of the LAO wafer or substituting the LAO single crystal with thin films. Furthermore, the same ideas can be generalized to develop the DUV photodetectors with the wide bandgap materials, such as LiTaO₃, MgO, ZrO₂, and so on.

This work is supported by the National Basic Research Program of China and the National Natural Science Foundation of China (NSFC).

References

1. H. Jiang and T. Egawa, "Low-dark-current high-performance AlGa_xN solar-blind p-i-n photodiodes," *Jpn. J. Appl. Phys.* **47**, 1541–1543 (2008).
2. C. J. Collins, U. Chowdhury, M. M. Wong, B. Yang, A. L. Beck, R. D. Dupuis, and J. C. Campbell, "Improved solar-blind detectivity using an Al_xGa_{1-x}N heterojunction p-i-n photodiode," *Appl. Phys. Lett.* **80**, 3754–3756 (2002).
3. P. Sandvik, K. Mi, F. Shahedipour, R. McClintock, A. Yasan, P. Kung, and M. Razeghi, "Al_xGa_{1-x}N for solar-blind UV detectors," *J. Cryst. Growth* **231**, 366–370 (2001).
4. A. Soltani, H. A. Barkad, M. Mattalah, B. Benbakhti, J.-C. De Jaeger, Y. M. Chong, Y. S. Zou, W. J. Zhang, S. T. Lee, A. BenMoussa, B. Giordanengo, and J.-F. Hochedez, "193 nm deep-ultraviolet solar-blind cubic boron nitride based photodetectors," *Appl. Phys. Lett.* **92**, 053501 (2008).
5. Y. Koide, M. Liao, and J. Alvarez, "Thermally stable solar-blind diamond UV photodetector," *Diam. Rel. Mater.* **15**, 1962–1966 (2006).
6. M. Bevilacqua and R. B. Jackman, "Extreme sensitivity displayed by single crystal diamond deep ultraviolet photoconductive devices," *Appl. Phys. Lett.* **95**, 243501 (2009).
7. Z. G. Ju, C. X. Shan, D. Y. Jiang, J. Y. Zhang, B. Yao, D. X. Zhao, D. Z. Shen, and X. W. Fan, "Mg_xZn_{1-x}O-based photodetectors covering the whole solar-blind spectrum range," *Appl. Phys. Lett.* **93**, 173505 (2008).
8. J. Xing, E. J. Guo, K. J. Jin, H. B. Lu, J. Wen, and G. Z. Yang, "Solar-blind deep-ultraviolet photodetectors based on an LaAlO₃ single crystal," *Opt. Lett.* **34**, 1675–1677 (2009).
9. E. J. Guo, J. Xing, H. B. Lu, K. J. Jin, J. Wen, and G. Z. Yang, "Ultraviolet fast-response photoelectric effects in LiTaO₃ single crystal," *J. Phys. D* **43**, 015402 (2010).
10. Y. Z. Chiou and J. J. Tang, "GaN photodetectors with transparent indium tin oxide electrodes," *Jpn. J. Appl. Phys.* **43**, 4146–4149 (2004).
11. M. L. Lee, P. F. Chi, and J. K. Sheu, "Photodetectors formed by an indium tin oxide/zinc oxide/p-type gallium nitride heterojunction with high ultraviolet-to-visible rejection ratio," *Appl. Phys. Lett.* **94**, 013512 (2009).
12. W. S. Jahng, A. H. Francis, H. Moon, J. I. Nanos, and M. D. Curtis, "Is indium tin oxide a suitable electrode in organic solar cells? Photovoltaic properties of interfaces in organic p/n junction photodiodes," *Appl. Phys. Lett.* **88**, 093504 (2006).
13. G. Z. Yang, H. B. Lu, F. Chen, T. Zhao, and Z. H. Chen, "Laser molecular beam epitaxy and characterization of perovskite oxide thin films," *J. Cryst. Growth* **227**, 929 (2001).
14. P. W. Peacock and J. Robertson, "Band offsets and Schottky barrier heights of high dielectric constant oxides," *J. Appl. Phys.* **92**, 4712–4721 (2002).